Study by *X*-Ray Crystallography and Mössbauer Spectroscopy of the Hexacyanoferrate(III) Compounds $Cs_2M[Fe(CN)_6]$ (M = Li, Na, or K)

By **Steven R. Fletcher** and **T. C. Gibb,*** Department of Inorganic and Structural Chemistry, The University, Leeds LS2 9JT

The crystal structures of $Cs_2Na[Fe(CN)_6]$ (I) and $Cs_2K[Fe(CN)_6]$ (II) have been elucidated by single-crystal *X*-ray analysis and compared with that of $Cs_2Li[Fe(CN)_6]$. Crystals of both are monoclinic, space group $P2_1/n$, with $Z = 2$ in unit cells of dimensions: (I), $a = 10.870(1)$, $b = 7.709(1)$, $c = 7.573(1)$ Å, $\beta = 89.994(6)°$; (II), $a = 11.140(1)$, $b = 8.131(1)$, $c = 7.660(1)$ Å, $\beta = 90.165(7)°$. The Mössbauer spectra of the series are discussed with particular reference to lattice dynamics, and to electronic spin-relaxation of the t_{2g}^5 $S = \frac{1}{2}$ configuration.

POTASSIUM hexacyanoferrate(III), $K_3[Fe(CN)_6]$, has been extensively studied [1] as the prototype material for the $^2T_2$ (t_{2g}^5) configuration of low-spin iron(III). However, the symmetry of the ligand field at the iron site is only rhombic, and in consequence the compound is difficult to study. The recently prepared [2] compound $Cs_2Li[Fe(CN)_6]$ has a cubic $Fm3m$ structure in which Li^+ and $[Fe(CN)_6]^{3-}$ ions occupy alternate corners of a cube and Cs^+ ions occupy the body centres. The structure [3] of $K_3[Fe(CN)_6]$ can be considered as a highly distorted version of this cubic lattice, and presents the possibility that other double salts might exist which are less distorted with perhaps a tetragonal symmetry at the iron site. This paper reports the preparation and crystal structures of $Cs_2Na[Fe(CN)_6]$ and $Cs_2K[Fe(CN)_6]$, and a detailed study by Mössbauer spectroscopy of the series $Cs_2M[Fe(CN)_6]$ (M = Li, Na, and K).

EXPERIMENTAL

All three compounds were prepared from $K_3[Fe(CN)_6]$, the appropriate cations being introduced by ion-exchange separations,[2] and were crystallised from aqueous solution. $Cs_2Na[Fe(CN)_6]$ proved to be comparatively insoluble. The sample of $Cs_2Li[Fe(CN)]_6$ was examined by *X*-ray powder diffraction and found to have the $Fm3m$ structure as published [2] with no impurity lines. The stoicheiometry of $Cs_2Na[Fe(CN)_6]$ was initially characterised by a caesium analysis {Found: Cs, 52.7. $Cs_2Na[Fe(CN)_6]$ requires 53.2%}, and that of $Cs_2K[Fe(CN)_6]$ by allowing it to react with excess of KI and titrating the liberated iodine {Found: $[Fe(CN)_6]^{3-}$, 41.2. $Cs_2K[Fe(CN)_6]$ requires 41.0%}.

Mössbauer spectra were recorded in the temperature range 4.2—295 K by use of a Ricor MCH 5 variable-temperature cryostat, and calibrated by use of an enriched iron metal foil at room temperature.

Both $Cs_2Na[Fe(CN)_6]$ and $Cs_2K[Fe(CN)_6]$ crystallise as good optical quality yellow polyhedra. Preliminary rotation and Weissenberg photographs showed that the crystal lattices of both compounds were very closely related to that of the cubic $Cs_2Li[Fe(CN)_6]$.[2] More careful inspection, however, revealed that in both cases the symmetry was lowered to monoclinic. The unique axis and one other are related to the 'cubic' repeat distance by a factor of *ca.* $1/\sqrt{2}$, giving a monoclinic unit cell of half the volume of the pseudocubic cell. Accurate unit-cell dimensions were obtained by a least-squares fit of sinθ values (30 for each crystal) measured on a diffractometer.

Crystal Data.—(*a*) $C_6Cs_2FeN_6Na$ (I), $M = 500.8$, Monoclinic, $a = 10.870(1)$, $b = 7.709(1)$, $c = 7.573(1)$ Å, $\beta = 89.994(6)°$, $U = 634.6$ Å^3, $Z = 2$, $D_c = 2.62$ g cm^{-3}. Space-group $P2_1/n$. Cu-K_{α_1} radiation, $\lambda = 1.540\,51$ Å; μ(Cu-K_{α_1}) = 541.8 cm^{-1}.

(*b*) $C_6Cs_2FeKN_6$ (II), $M = 516.9$, Monoclinic, $a = 11.140(1)$, $b = 8.131(1)$, $c = 7.660(1)$ Å, $\beta = 90.165(7)°$, $U = 693.8$ Å^3, $Z = 2$, $D_c = 2.47$ g cm^{-3}. Space-group $P2_1/n$. μ(Cu-K_{α_1}) = 518.3 cm^{-1}.

The crystals selected for intensity data collection measured *ca.* 0.2 × 0.15 × 0.1 (I) and 0.3 × 0.3 × 0.1 (II) mm respectively. Data were measured on a Nonius CAD 4 automatic four-circle diffractometer by use of monochromatised Cu-K_{α_1} radiation. Intensities were recorded in the θ—2θ scan mode using a scintillation counter and pulse-height discrimination. Control reflections, measured at intervals of 50 reflections during both data collections, did not vary by $>\pm 2\%$. In the case of $Cs_2Na[Fe(CN)_6]$ a total of 1 202 independent reflections (to θ 70°) was measured, of which 897 having $I > 2.58\sigma(I)$ were considered observed, where $I = P - 2(B_1 + B_2)$ and $\sigma^2(I) = P + 4(B_1 + B_2) + (0.05I)^2$. For $Cs_2K[Fe(CN)_6]$ these values were 1 315 independent reflections measured and 1 118 observed. The intensities were corrected for Lorentz and polarisation factors.

Solution and Refinement of the Structure.—The structures were solved by using metal-atom co-ordinates derived from the structure of $Cs_2Li[Fe(CN)_6]$ as starting parameters for least-squares refinement. From subsequent difference-Fourier syntheses the carbon and nitrogen atoms were located. Inclusion of these in the isotropic least-squares refinement gave *R* factors of 0.127 (I) and 0.061 (II). Data were now corrected for absorption by use of the Gaussian integration technique [4] with crystal pathlengths determined by a vector-analysis procedure.[5] Refinement as before gave *R* 0.111 (I) and 0.110 (II). When the metal atoms were allowed to refine with anisotropic thermal parameters *R* values were reduced to 0.090 and 0.094, and a fully anisotropic refinement converged with *R* 0.067 (I) and 0.083 (II). Finally an extinction correction was applied,[6] the coefficient *g* being varied in the least-squares refinement. Final values of *g* were 5.6×10^{-4} and 8.6×10^{-4} respectively, and the final *R* factors 0.060 and 0.075. The reflections were assigned weights of $1/\sigma^2$ in the least-squares refinement, derived from the expression for σ already given.

Full-matrix least-squares refinement was used throughout. Atomic scattering factors were from ref. 7, and the real and imaginary parts of the anomalous dispersion corrections for the metal atoms were from ref. 8. Calculations were carried out using the University of Leeds ICL

[1] W. T. Oosterhuis and G. Lang, *Phys. Rev.*, 1969, **178**, 439.
[2] B. I. Swanson and R. R. Ryan, *Inorg. Chem.*, 1973, **12**, 283.
[3] B. N. Figgis, M. Gerloch, and R. Mason, *Proc. Roy. Soc.*, 1969, **A309**, 91.
[4] W. R. Busing and H. A. Levy, *Acta Cryst.*, 1957, **10**, 180.
[5] P. Coppens, L. Leiserowitz, and D. Rabinovich, *Acta Cryst.*, 1965, **18**, 1035.
[6] W. H. Zachariasen, *Acta Cryst.*, 1967, **23**, 558.
[7] D. T. Cromer and J. T. Waber, *Acta Cryst.*, 1965, **18**, 104.
[8] D. T. Cromer, *Acta Cryst.*, 1965, **18**, 17.

1906A and the University of Manchester CDC 7600 computers with programs listed in ref. 9.

Table 1 lists the final fractional co-ordinates with their estimated standard deviations. The coefficients in the expression for the anisotropic temperature factor, $\exp[-2\pi^2(U_{11}h^2a^{*2} + U_{22}k^2b^{*2} + U_{33}l^2c^{*2} + 2U_{12}hka^*b^* + 2U_{13}hla^*c^* + 2U_{23}klb^*c^*)]$, and the root-mean-square amplitudes of vibration along the principal axes of the thermal ellipsoid are listed, together with observed and calculated structure amplitudes, in Supplementary Publication No. SUP 21901 (15 pp., 1 microfiche).*

TABLE 1

Fractional co-ordinates, with estimated standard deviations in parentheses

	x	*y*	*z*
(*a*) $Cs_2Na[Fe(CN)_6]$, (I)			
Cs	0.249 96(8)	0.459 60(11)	−0.009 18(11)
Na	0.0	0.5	0.5
Fe	0.0	0.0	0.0
C(1)	0.019 2(10)	0.142 2(14)	−0.205 9(13)
C(2)	0.024 2(9)	−0.205 4(14)	−0.143 5(13)
C(3)	0.174 7(10)	0.006 1(14)	0.040 5(14)
N(1)	0.032 8(11)	0.227 4(14)	−0.329 9(13)
N(2)	0.037 8(10)	−0.323 2(14)	−0.230 7(12)
N(3)	0.278 7(9)	0.014 7(16)	0.068 0(16)
(*b*) $Cs_2K[Fe(CN)_6]$, (II)			
Cs	0.250 55(7)	0.432 51(10)	−0.020 65(11)
K	0.0	0.5	0.5
Fe	0.0	0.0	0.0
C(1)	0.029 6(10)	0.128 0(15)	−0.207 6(14)
C(2)	0.038 7(11)	−0.199 1(14)	−0.123 4(13)
C(3)	0.165 4(10)	0.019 3(15)	0.068 3(15)
N(1)	0.049 7(12)	0.203 1(14)	−0.332 6(14)
N(2)	0.060 8(12)	−0.319 8(15)	−0.197 2(15)
N(3)	0.262 9(10)	0.035 7(15)	0.113 1(17)

DESCRIPTION OF THE STRUCTURES AND DISCUSSION

Figures 1 and 2 † show the crystal structures of $Cs_2Na[Fe(CN)_6]$, (I), and $Cs_2K[Fe(CN)_6]$, (II), in projection down the *a* and *b* axes. More important interatomic distances and angles are listed in Table 2. Both structures are similar to that [2] of the cubic $Cs_2Li[Fe(CN)_6]$ but there is a lowering of symmetry and a progressive distortion as the lithium ion is replaced by first sodium and then potassium. In both cases the iron atom and the smaller alkali-metal cation occupy inversion centres in the space group $P2_1/n$, while the caesium ion and the cyano-ligands are in general positions.

The lower symmetry in these structures clearly results from distortion due to the different sizes of the cations substituted for lithium. This distortion may be considered as a combination of three concerted effects. In both cases the unit cell, which is pseudo-tetragonal with the pseudo-four-fold axis parallel to the crystallographic *a* axis, has *b* slightly longer than *c*, such that $b > a/\sqrt{2} > c$. The caesium ions, initially positioned at (1/4,1/2,0) as derived from the cubic structure, moved away from these positions during the course of least-squares refinement by 0.32 Å for the Na and 0.57 Å for the K salt. In addition the hexacyanoferrate ions are forced to rotate to adopt a favourable orientation between the alkali-metal cations. This rotation may be defined by the angles made by each of the three independent Fe–C–N vectors with the closest crystallographic axis. These angles are 10.1, 34.9, and 36.3° (Na) and 16.5, 33.0, and 34.3° (K) relative to the *a*, *b*, and *c* axes respectively. In a situation approaching cubic symmetry these angles would, of course, tend to 0, 45, and 45°.

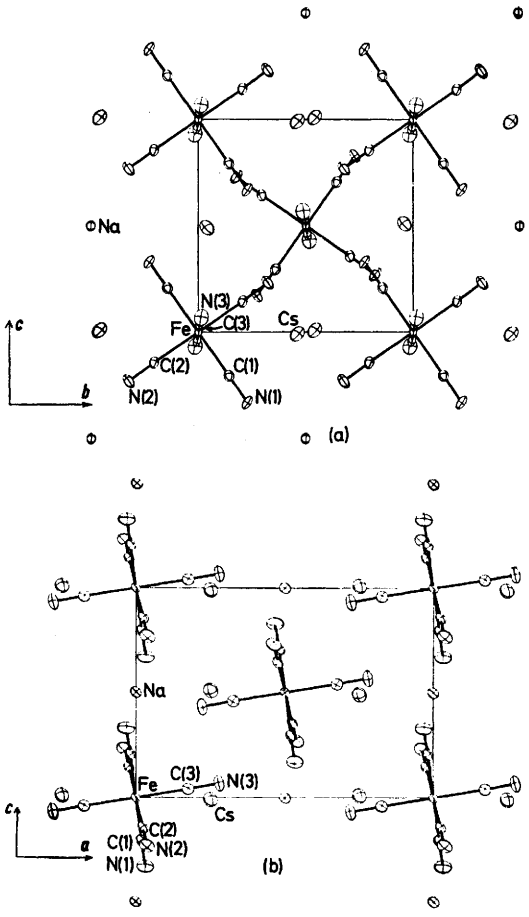

FIGURE 1 The structure of $Cs_2Na[Fe(CN)_6]$ viewed in projection along (a) the *a*, and (b) the *b* axis. Thermal ellipsoids are scaled to enclose 50% probability

There appears to be much less free space in the two crystal structures reported here than in $Cs_2Li[Fe(CN)_6]$.[2] There the caesium ion occupies too large a cavity, with the Cs · · · N distance being 3.762 Å. In both the Na and K salts, however, the Cs · · · N distances are much closer to the sum of the combined atomic radii (3.24 Å).[10] The Na · · · N and K · · · N distances are also near to the predicted values (2.45 and 2.85 Å). While the Li structure is basically held together by strong Li–N bonds,

* See Notice to Authors No. 7 in *J.C.S. Dalton*, 1976, Index issue.

† In Figures 1(a) and 2(a) the Na and K ions, as given in Table 1, are hidden by the iron atom in the centre of the projection.

[9] '*X*-Ray '70,' system of programs, eds. J. M. Stewart, F. A. Kundell, and J. C. Baldwin, 1970 revision of University of Maryland Technical Report 67–58; also 1972 version, Technical Report TR 192.

[10] J. C. Slater, *J. Chem. Phys.*, 1964, **41**, 3199.

it would seem that in the present structures there are bonds from the cyano-ligands to both alkali-metal cations. It is interesting that the K · · · N distances in $Cs_2K[Fe(CN)_6]$ are all less than the mean K · · · N distance of 3.03 Å in $K_3[Fe(CN)_6]$.[3]

There is no significant distortion from octahedral geometry in the hexacyanoferrate ion, and the Fe–C and

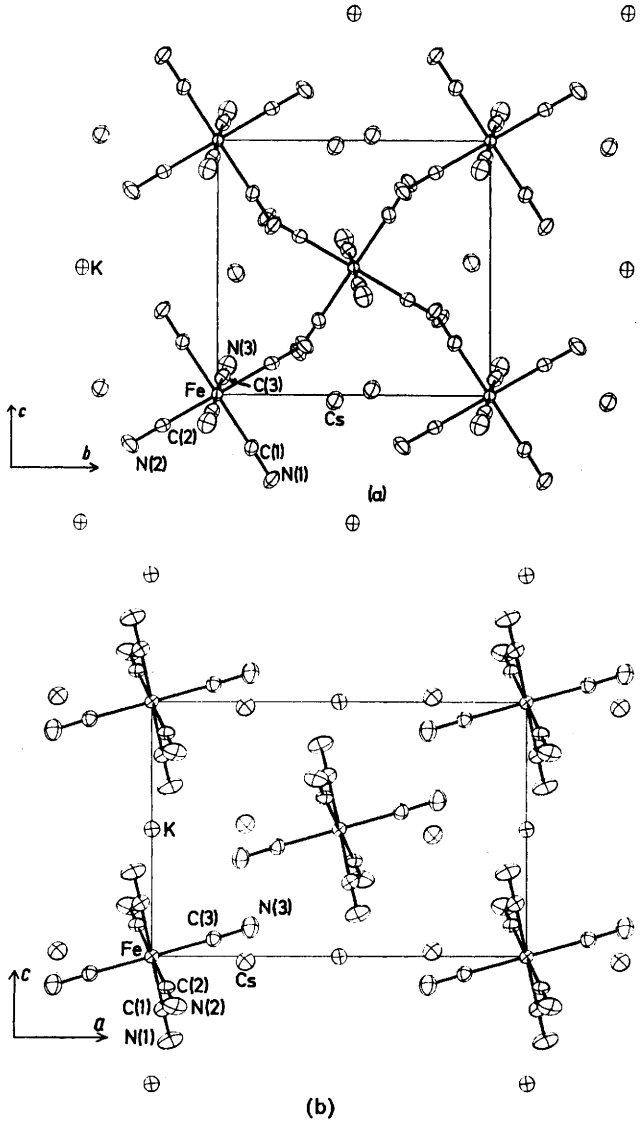

FIGURE 2 The structure of $Cs_2K[Fe(CN)_6]$ viewed in projection along (a) the *a*, and (b) the *b* axis. Thermal ellipsoids are scaled to enclose 50% probability

C–N bond distances are in good agreement with those in $Cs_2Li[Fe(CN)_6]$ and $K_3[Fe(CN)_6]$. As shown later, it seems most probable that the principal factor causing the observed splitting in the Mössbauer spectra is the unsymmetrical caesium environment of the iron atoms. In $Cs_2Li[Fe(CN)_6]$ each iron atom is surrounded by eight caesium ions at the corners of a cube. In the present two structures that cube has become distorted to a parallelepiped with Fe · · · Cs distances varying between 4.466 and 4.974 Å in $Cs_2Na[Fe(CN)_6]$ and between 4.493 and 5.395 Å in $Cs_2K[Fe(CN)_6]$.

Although the symmetry of the lattice is lowered from cubic to monoclinic when lithium ions are substituted by sodium or potassium, the monoclinic β angles remain very close to 90°, indeed not significantly different in the case of $Cs_2Na[Fe(CN)_6]$. This may be compared with the situation in $K_3[Fe(CN)_6]$ [3] which crystallises in the monoclinic space group $P2_1/c$, with one potassium ion in a general position and one on an inversion centre, and with a unit cell of similar axial lengths to those in the present study. However, in $K_3[Fe(CN)_6]$ the longest axis is the unique monoclinic *b* axis, and the β angle is 107°.

TABLE 2

Interatomic distances (Å) and angles (°) for $Cs_2M[Fe(CN)_6]$ with estimated standard deviations in parentheses

M	Li*	Na	K
Fe–C(1)		1.917(10)	1.930(11)
Fe–C(2)	1.926(3)	1.939(10)	1.924(11)
Fe–C(3)		1.924(11)	1.921(11)
C(1)–N(1)		1.155(14)	1.158(16)
C(2)–N(2)	1.148(5)	1.133(15)	1.159(17)
C(3)–N(3)		1.152(15)	1.146(16)
C(1)–Fe–C(2)		89.8(4)	90.6(5)
C(1)–Fe–C(3)	90	90.5(4)	90.8(5)
C(2)–Fe–C(3)		89.5(4)	89.2(5)
Fe–C(1)–N(1)		178.8(10)	178.5(11)
Fe–C(2)–N(2)	180	178.4(10)	179.2(11)
Fe–C(3)–N(3)		177.7(11)	177.4(11)
Cs · · · N(2^{I})		3.307(11)	3.215(13)
Cs · · · N(3)		3.493(13)	3.388(13)
Cs · · · N(3^{II})	3.762(1)	3.382(12)	3.237(13)
Cs · · · N(1^{III})		3.365(11)	3.327(12)
M · · · N(2^{IV})		2.487(10)	2.824(12)
M · · · N(1^{V})	2.212(3)	2.491(10)	2.789(11)
M · · · N(3^{II})		2.462(10)	2.797(11)

* From ref. 1. Roman numeral superscripts refer to atoms in the following positions:

I $x, 1+y, z$ IV $x, 1+y, 1+z$
II $\frac{1}{2}-x, \frac{1}{2}+y, \frac{1}{2}-z$ V $x, y, 1+z$
III $\frac{1}{2}-x, \frac{1}{2}+y, -\frac{1}{2}-z$

MÖSSBAUER SPECTRA AND DISCUSSION

Typical Mössbauer spectra of the three compounds are shown in Figures 3—5. At 292 K the Mössbauer spectrum of $Cs_2Li[Fe(CN)_6]$ comprises a single line appropriate to strict O_h symmetry of the $[Fe(CN)_6]^{3-}$ anion as indicated by the $Fm3m$ crystal structure. However, the t_{2g}^5 configuration is in principle subject to a weak Jahn–Teller effect, and the possibility of a distortion or phase change at low temperatures was examined. A gradual broadening of the resonance line begins at *ca.* 200 K (Figure 6), but as shown later this can be attributed entirely to spin-lattice relaxation, and is unlikely to be due to quadrupole splitting from a small distortion. The linewidth increased from 0.29 mm s^{-1} at 292 K to 0.43 mm s^{-1} at 87 K, but an exploratory measurement at 4.2 K confirmed that there is no further broadening or significant change in the spectrum below 87 K.

In contrast, $Cs_2Na[Fe(CN)_6]$ shows a small temperature-dependent quadrupole splitting. This is clearly

seen at low temperatures, but is barely resolved at 293 K (Figure 4). Each spectrum was curve-fitted with two Lorentzian lines constrained to have equal widths and intensities. This procedure resulted in values for the quadrupole splitting (Figure 7) and linewidths (Figure 6) which were self-consistent. Although the finite thickness of the absorber will introduce a small systematic

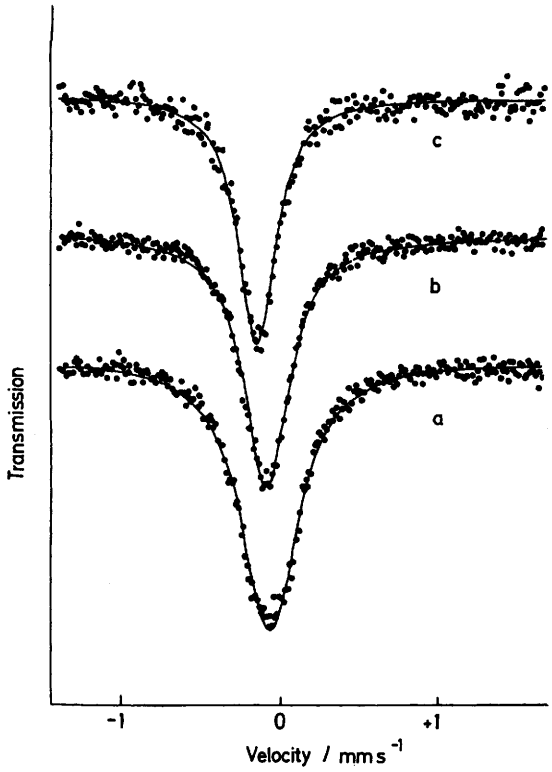

FIGURE 3 Mössbauer spectra of $Cs_2Li[Fe(CN)_6]$ at (a) 87, (b) 162, and (c) 292 K

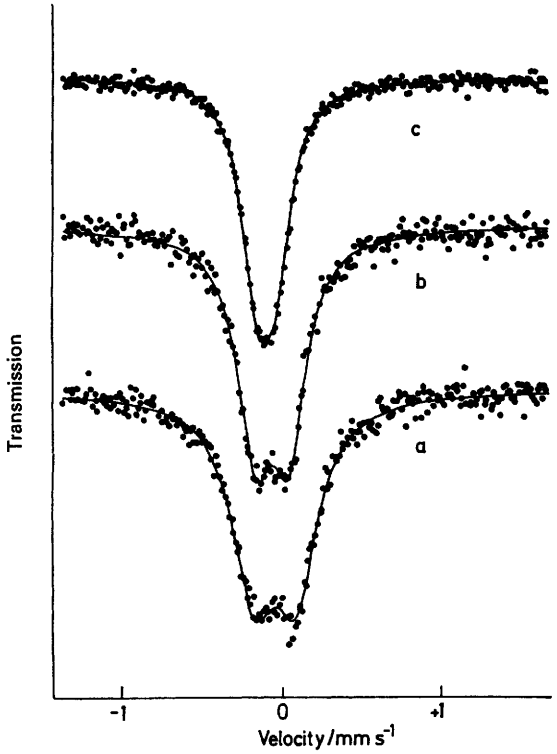

FIGURE 4 Mössbauer spectra of $Cs_2Na[Fe(CN)_6]$ at (a) 84, (b) 162, and (c) 293 K

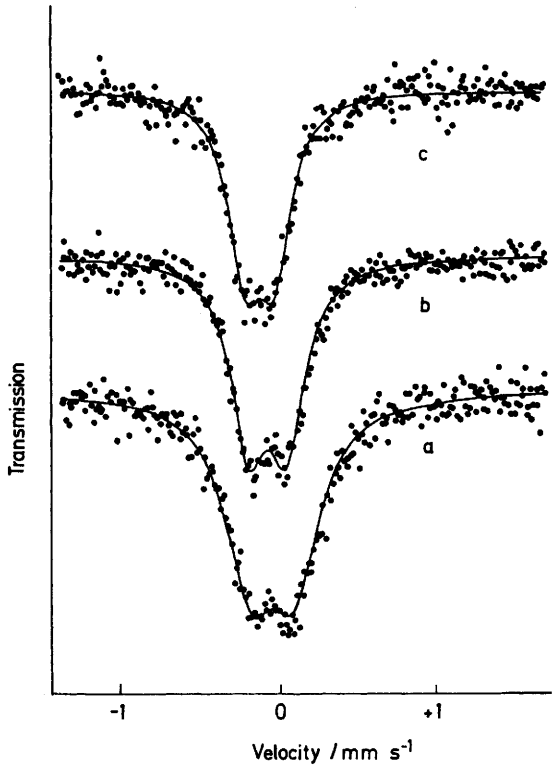

FIGURE 5 Mössbauer spectra of $Cs_2K[Fe(CN)_6]$ at (a) 87, (b) 162, and (c) 293 K

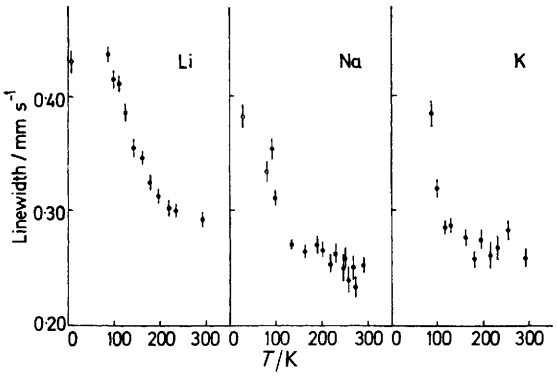

FIGURE 6 The experimental linewidth of the Mössbauer spectrum of $Cs_2M[Fe(CN)_6]$ (M = Li, Na, or K) as a function of temperature. (Values shown as open circles were obtained using a different absorber and are therefore not fully self-consistent with the other data)

error because of saturation, it is considered that a more accurate 'transmission-integral' analysis is an unnecessary complication, and in practice the absorbers were made as thin as possible to minimise the errors. The spectra of $Cs_2K[Fe(CN)_6]$ are similar, but with a more pronounced splitting. The presence of a temperature-dependent quadrupole splitting in these two

compounds confirms the non-cubic symmetry of the ligand field at the iron site.

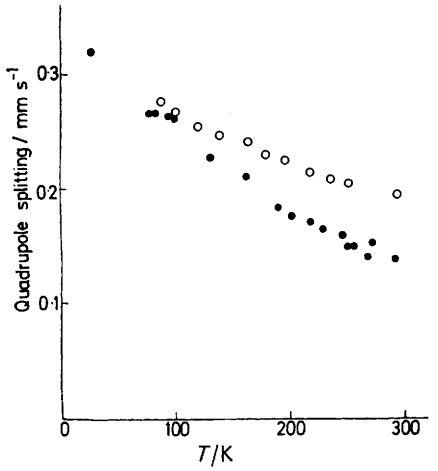

FIGURE 7 Temperature-dependence of quadrupole splitting in $Cs_2Na[Fe(CN)_6]$ and $Cs_2K[Fe(CN)_6]$; open circles K, closed circles Na

Lattice Dynamics.—A self-consistent set of data for the temperature dependence of the spectrum area was obtained for each compound (Figure 8), together with values for the chemical isomer shift (Figure 9; with respect to Fe metal at room temperature). These can be related to the lattice dynamical properties of the resonant nucleus.

The recoilless fraction f (which for a thin absorber is related linearly to the spectrum area) is determined by the mean-square vibrational amplitude $\langle x^2 \rangle$ such that $f = \exp\{-E_\gamma^2\langle x^2\rangle/(\hbar c)^2\}$, where E_γ is the energy of the γ ray, c is the velocity of light, and $\hbar$ is Planck's constant. The second-order Doppler shift, $\delta E/E_\gamma$, which accounts for the temperature-dependence of the chemical-isomer shift (neglecting thermal expansion effects) is related to the mean-square velocity $\langle v^2 \rangle$: $\delta E/E_\gamma = -\langle v^2\rangle/2c^2$.

In a molecular solid it is often found that $\langle x^2 \rangle$ is weighted towards the lower frequencies (*i.e.* the lattice or intermolecular vibrations) while $\langle v^2 \rangle$ is weighted towards the higher frequencies (*i.e.* the intramolecular vibrations). For this reason Hazony devised a simple two-frequency model [11] which he applied to experimental data for $K_4[Fe(CN)_6]$, and in view of the similar nature of the new compounds it is interesting to consider them by use of the same model.

Following his nomenclature the low and high frequencies and the corresponding ' lattice temperatures ' are denoted by $\hbar\omega_l = k\theta_l$ and $\hbar\omega_h = k\theta_h$ respectively.

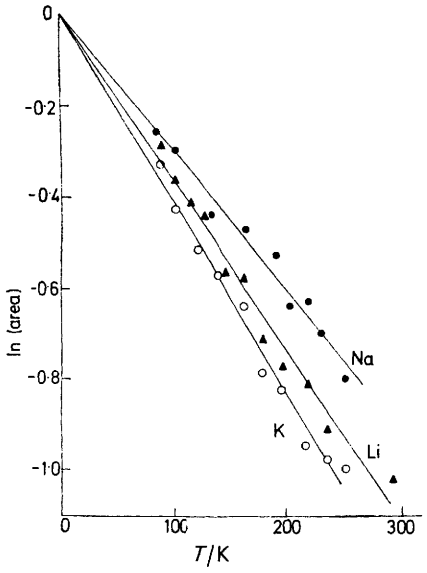

FIGURE 8 Temperature-dependence of spectrum area for $Cs_2M[Fe(CN)_6]$ (M = Li, Na, or K). Solid lines are a least-squares fit

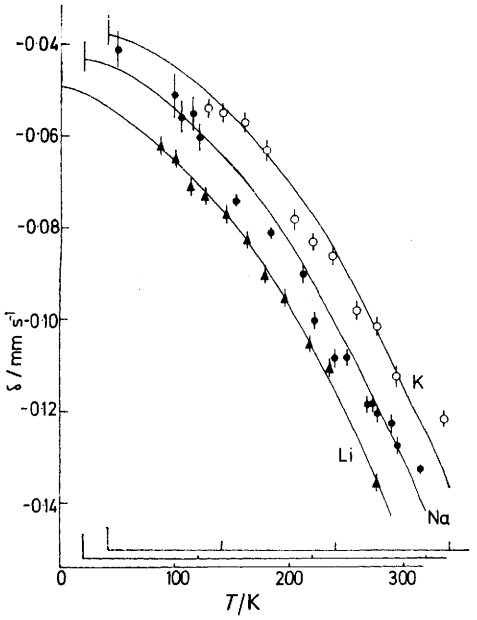

FIGURE 9 Temperature-dependence of the chemical-isomer shift. Solid lines represent a theoretical fit using a two-frequency model

At intermediate temperature where $\theta_l < T < \theta_h$ it is possible to show [11] that:

$$\frac{d}{dT}\ln f \simeq -(kE_\gamma^2/M'c^2)[1/(k\theta_l)^2]$$

and

$$\delta E/E_\gamma = -\tfrac{3}{2}E_\gamma[(k\theta_l/M'c^2)(\tfrac{1}{2} + \eta_l) + (k\theta_h/M''c^2)(\tfrac{1}{2} + \eta_h)]$$

where $\eta_l = [\exp(\theta_l/T) - 1]^{-1}$, M' is the molecular mass, M is the mass of the resonant nucleus, and $M'' = M'M/(M' - M)$.

The linear dependence of $\ln f$ (and hence the spectrum area) on temperature can be used directly to determine the lattice temperature θ_l. The data of Figure 8 have been analysed in this way, giving values for θ_l in $Cs_2Li[Fe(CN)_6]$ (57 K), $Cs_2Na[Fe(CN)_6]$ (63 K), and $Cs_2K[Fe(CN)_6]$ (54 K). Although the variations are comparatively small, the higher value for the sodium compound is commensurate with its lower solubility and presumably higher lattice energy. The value

[11] Y. Hazony, *J. Chem. Phys.*, 1966, **45**, 2664.

obtained by Hazony [11] for $K_4[Fe(CN)_6]$ was 75 K, which presumably is higher because of the increase in overall charge on the anion.

The values of θ_l were used to deduce θ_h from the chemical-isomer shift data. In all three compounds a value of θ_h 650 $\pm$ 50 K was found, compared to a similar value of 700 $\pm$ 50 K in $K_4[Fe(CN)_6]$. When the zero-point motion is taken into account by extrapolation of the observed shift data to 0 K using the experimental values for θ_h and θ_l, it is possible to calculate 'true' values for the chemical-isomer shift. The extrapolated values at 0 K are −0.049, −0.043, and −0.038 mm s^{-1}, and the 'true values' are 0.129, 0.135, and 0.140 mm s^{-1} for $Cs_2Li[Fe(CN)_6]$, $Cs_2Na[Fe(CN)_6]$, and $Cs_2K[Fe(CN)_6]$ respectively. The small progressive increase along the series is a reflection of the decreasing covalency of the cation with the anion, although the mechanism by which this influences the iron atom can only be conjectured. The corresponding 'true' value in $K_4[Fe(CN)_6]$ is 0.441 mm s^{-1}, which is much larger, as expected for the change in oxidation state.

Spin-relaxation and Line-broadening.—The line-broadening seen in all three compounds can be attributed to slow relaxation of the electron spin [the t_{2g}^5 configuration of iron(III) has $S = \frac{1}{2}$]. The relaxation is caused by the combined effects of spin-lattice relaxation (correlation time τ_L) and spin–spin relaxation (τ_S), and the effective correlation time is given by: $1/\tau = 1/\tau_L + 1/\tau_S$.

In most circumstances τ_S is independent of temperature and τ_L increases with decreasing temperature. It is therefore possible to attribute the initial broadening to the slowing down of spin-lattice relaxation. Both $Cs_2Li[Fe(CN)_6]$ and $Cs_2Na[Fe(CN)_6]$ were shown to have an effectively constant linewidth below 80 K, and similar effects have been recorded [1] in $K_3[Fe(CN)_6]$. This limiting behaviour is determined by the values of τ_S.

The problem of spin-relaxation broadening in a single-line absorber with no quadrupole interaction has been treated by Bradford and Marshall.[12] The hyperfine interaction for the nuclear ground-state spin I with the electron spin S is given by: $\mathscr{H}_g = A\boldsymbol{I} \cdot \boldsymbol{S}$ and is isotropic so that A can be treated as a scalar. With their nomenclature and writing the corresponding equation for the nuclear excited-state spin J as $\mathscr{H}_e = A'\boldsymbol{J} \cdot \boldsymbol{S}$, the final expression for the absorption as a function of frequency ω is given by their equation 3.16 as:

$$A(\omega) \simeq \left\{ \frac{\Gamma + b/R}{\omega^2 + (\Gamma + b/R)^2} \exp\left(\frac{b}{R^2}\right) - \frac{b}{R^2} \frac{(\Gamma + R)}{[\omega^2 + (\Gamma + R)^2]} \right\}$$

where $b = [S(S+1)/3\hbar^2](\frac{3}{4}A^2 + \frac{15}{4}A'^2 - \frac{5}{2}AA')$, 2Γ is the unbroadened natural linewidth, and R is the relaxation rate ($R = 1/\tau$). When b/R^2 is small, which applies in the present instance, then this equation may be reduced to: $A(\omega) \simeq (\Gamma + b/R)/[\omega^2 + (\Gamma + b/R)^2]$, which corresponds to a Lorentzian line of width: $2\Gamma_a = 2\Gamma + 2b/R$. Thus the linewidth varies directly as R^{-1} and increases at τ increases.

A and A' are in the ratio of the nuclear g-factors, and it is possible to relate the broadening quantitatively to the relaxation time. If we were to consider an $S = \frac{1}{2}$ ion in the effective-field approximation with very slow relaxation, so that $\mathscr{H} = A_Z\boldsymbol{I} \cdot \boldsymbol{S} = g\mu_N BI_Z$, then $A \simeq 2g\mu_N B$ where g is the nuclear g-factor and μ_N is the nuclear magneton. The effective magnetic-flux density, B, due to the $S = \frac{1}{2}$ state can be approximated by $B = -22\langle S_Z \rangle = -11$ T (this is an empirical value based on the observation that the saturation value of B is *ca.* −11 T per unpaired electron in many different iron compounds). This results in values of $A = 20.0 \times 10^{-27}$ J and $A' = -11.6 \times 10^{-27}$ J, so that $b/R = 1.10 \times 10^7\ \tau$ mm s^{-1} and $2\Gamma_a \simeq 2\Gamma + 2.20 \times 10^7\ \tau$ mm s^{-1}.

The temperature-dependence of τ_L is complex because it is compounded of three competing processes for spin–lattice relaxation.[13] Values of τ_L can be deduced from the experimental data in the region of intermediate broadening by using the low-temperature limiting value of τ_S. However, although it is clear that τ_L varies approximately as T^5, a more detailed analysis is not possible on the present data.

The relaxation time τ_S is determined by the dipole–dipole interaction of the electronic spin S on the resonant nucleus with all the other spins S_j and can be represented by the well-known formula:

$$\mathscr{H}_{dd} = \left(\frac{\mu_0}{4\pi}\right) g^2\beta^2 \sum_j \frac{1}{r_j^3} [(\boldsymbol{S} \cdot \boldsymbol{S}_j) - 3(\boldsymbol{S} \cdot \hat{\boldsymbol{r}}_j)(\boldsymbol{S}_j \cdot \hat{\boldsymbol{r}}_j)]$$

where g is the electronic g-value, r_j is the distance separating the j'th ion from the Mössbauer nucleus (with corresponding unit vector $\hat{\boldsymbol{r}}_j$), β is the Bohr magneton, and μ_0 is the permeability of a vacuum. This can be re-written as the sum of six terms:

$$\mathscr{H}_{dd} = \left(\frac{\mu_0}{4\pi}\right) g^2\beta^2 (A + B + C + D + E + F)$$

where

$$A = \sum_j \frac{1}{r_j^3} (1 - 3\cos^2\theta_j) S_z S_{jz}$$

$$B = -\tfrac{1}{4} \sum_j \frac{1}{r_j^3} (1 - 3\cos^2\theta_j)(S_+ S_{j-} + S_- S_{j+})$$

$$C = -\tfrac{3}{2} \sum_j \frac{1}{r_j^3} \sin\theta_j \cos\theta_j e^{-i\phi_j} (S_z S_{j+} + S_+ S_{jz})$$

$$E = -\tfrac{3}{4} \sum_j \frac{1}{r_j^3} \sin^2\theta_j e^{-2i\phi_j} S_+ S_{j+}$$

$$D = C^\dagger$$

$$F = E^\dagger$$

For the $^2T_2$ (t_{2g}^5) configuration in octahedral symmetry, the ground state is a Kramers' doublet which is *ca.* 300 cm^{-1} below the next excited state because of the large value of the spin-orbit coupling. At low temperatures the spin–spin relaxation can be considered as taking place within an $S_z = \pm\frac{1}{2}$ level. Energy-conserving

[12] E. Bradford and W. Marshall, *Proc. Phys. Soc.*, **1966**, **87**, 731.
[13] V. V. Svetozarov, *Soviet Phys. Solid State*, **1970**, **12**, 826.

transitions can be induced [14] by the terms C, D, E, and F in addition to the normal 'flip-flop' term B, and using the 'golden rule' of time-dependent perturbation theory [14,15] which gives the transition probability as being proportional to the square of the matrix element one obtains:

$$R_S = \frac{4\pi^2}{h} |\langle m'|\mathscr{H}_{dd}|m\rangle|^2 \rho$$

where

$$|\langle m'|\mathscr{H}_{dd}|m\rangle|^2 = \left(\frac{\mu_0}{4\pi} g^2\beta^2\right)^2 \tfrac{1}{16} \sum_j \frac{1}{r_j^6} \times [(1 - 3\cos^2\theta_j)^2 + 18\sin^2\theta_j \cos^2\theta_j + 9\sin^4\theta_j]$$

and ρ is a proportionality constant which has the dimensions of J^{-1} and can therefore be referred to as a 'density of states' parameter.

In the absence of a preferred orientation we can average over all θ to obtain: $R_S = \frac{5}{16}[(\mu_0^2 g^4\beta^4)/\hbar]\rho \sum_j \frac{1}{r_j^6}$. The relaxation rate is therefore dependent on the iron–iron distances (this explains why the low-temperature linewidths of $K_3[Fe(CN)_6]$, $Cs_2Li[Fe(CN)_6]$, and $Cs_2Na[Fe(CN)_6]$ are so similar). For $Cs_2Li[Fe(CN)_6]$ the value [16] of the isotropic g-value is 2, the value of $\sum_j 1/r_j^6$ is 8.279×10^{55} m^{-6}, and with the observed relaxation time at 4.2 K of $\tau \simeq 5 \times 10^{-9}$ s gives a value for the density of states, ρ, of 2.7×10^{22} J^{-1}.

In $Cs_2Na[Fe(CN)_6]$ and $Cs_2K[Fe(CN)_6]$ where a quadrupole interaction is present, the lineshape as a function of relaxation rate can be expressed by equations 4.8, 4.9, and 4.10 of ref. 12. The hyperfine interaction is no longer isotropic, and the equations given are appropriate to axial symmetry only, but are useful in the present context. The interaction is: $\mathscr{H} = AI_zS_z + B(I_xS_x + I_yS_y)$, where the z axis refers to the principal axis of the electric-field gradient tensor. The general expressions for the lineshape [12] can be simplified in certain limiting cases as follows.

If the hyperfine tensor is highly anisotropic such that $A \neq B = 0$ then the initial broadening can be represented by:

$$A_{\parallel}(\omega) = \frac{\Gamma + x/R}{(\omega - \lambda)^2 + (\Gamma + x/R)^2} + \frac{2}{3}\frac{\Gamma + y/R}{(\omega + \lambda)^2 + (\Gamma + y/R)^2} + \frac{1}{3}\frac{\Gamma + z/R}{(\omega + \lambda)^2 + (\Gamma + z/R)^2}$$

where $x = [S(S+1)/3\hbar^2](\frac{1}{4}A^2 + \frac{9}{4}A'^2 - \frac{3}{2}AA')$

$y = [S(S+1)/3\hbar^2](\frac{1}{4}A^2 + \frac{1}{4}A'^2 - \frac{1}{2}AA')$

$z = [S(S+1)/3\hbar^2](\frac{1}{4}A^2 + \frac{1}{4}A'^2 + \frac{1}{2}AA')$

and $2\lambda = e^2qQ/2$ is the quadrupole coupling constant. Taking $A'/A = g'/g$, the ratio of the nuclear g-factors ($= -0.104/0.1812$), we find $x\alpha(A - 3A')^2$, $y\alpha(A - A')^2$, $z\alpha(A + A')^2$ which are in the ratio $1 : 0.34 : 0.02$. Thus the $\pm\frac{1}{2}\rightarrow\pm\frac{3}{2}$ transition (at $\omega = \lambda$) broadens more rapidly than the $\pm\frac{1}{2}\rightarrow\pm\frac{1}{2}$, $\pm\frac{1}{2}\rightarrow\mp\frac{1}{2}$ transition (at $\omega = -\lambda$).

If, on the other hand, we have $B \neq A = 0$ (*i.e.* the field is perpendicular to z) an essentially similar equation is obtained but with

$x = [S(S+1)/3\hbar^2](\frac{1}{2}B^2 + \frac{3}{2}B'^2)$

$y = [S(S+1)/3\hbar^2](\frac{1}{2}B^2 + \frac{7}{2}B'^2 - 2BB')$

$z = [S(S+1)/3\hbar^2](\frac{1}{2}B^2 + \frac{7}{2}B'^2)$

So that $x\alpha(B^2 + 3B'^2)$, $y\alpha(B^2 + 7B'^2 - 4BB')$, $z\alpha(B^2 + 7B'^2)$ which with $B'/B = g'/g$ gives the ratios $0.35 : 1 : 0.59$. Thus in this instance the $\pm\frac{1}{2}\rightarrow\pm\frac{3}{2}$ transition broadens more slowly, but the asymmetry is less marked. These results can be predicted independently from the stochastic theory of relaxation by Blume and Tjon.[17] However, the intermediate situation where $A \neq B \neq 0$ can only be treated using the perturbation equation.[12]

If for example we again consider $A = B \neq 0$ then the initial broadening can be described with:

$x = [S(S+1)/3\hbar^2](\frac{3}{4}A^2 + \frac{15}{4}A'^2 - \frac{3}{2}AA')$

$y = [S(S+1)/3\hbar^2](\frac{3}{4}A^2 + \frac{15}{4}A'^2 - \frac{5}{2}AA')$

$z = [S(S+1)3\hbar^2](\frac{3}{4}A^2 + \frac{15}{4}A'^2 + \frac{1}{2}AA')$

which are in the ratios $0.53 : 0.24 : 1$. The two lines will broaden more evenly and more rapidly.

Note that anisotropy in the hyperfine interaction results in a slower initial broadening which becomes asymmetric. The fact that broadening commences at a higher temperature in $Cs_2Li[Fe(CN)_6]$ may therefore be attributed, at least in part, to the fact that the relaxation is isotropic, and need not imply a significant difference in the spin-lattice relaxation rates. However, the comparatively symmetric broadening in $Cs_2Na[Fe(CN)_6]$ and $Cs_2K[Fe(CN)_6]$ suggests that the hyperfine tensor is of the form $A \neq B \neq 0$, and that it is not possible to deduce values of τ_L from the line-broadening without further information about the relative magnitudes of A and B. However, the indications are that A and B are approximately equal because the low-temperature spectra in Figures 4 and 5 are symmetrical within experimental error.

Ligand-field Considerations.—The quadrupole splitting is produced by a combination of two effects. A non-cubic array of ionic charges external to the atom can produce a finite contribution to the electric-field gradient tensor which is only weakly temperature-dependent (by thermal expansion). Secondly, the electronic configuration of the resonant atom is a t_{2g}^5 configuration which gives three Kramers' doublets in the ligand field as a result of spin–orbit coupling; although there is no electric-field gradient in a cubic ligand-field, distortion of the $[Fe(CN)_6]^{3-}$ unit will cause state mixing and a gradient which is strongly temperature-dependent because of thermal population of the levels.[18]

[14] S. Dattagupta, *Phys. Rev. B.*, 1975, **12**, 3584.
[15] M. Blume, *Phys. Rev. Letters*, 1967, **18**, 305.
[16] H. Kamimura, *J. Phys. Soc. Japan*, 1956, **11**, 1171.
[17] M. Blume and J. A. Tjon, *Phys. Rev.*, 1968, **165**, 446.

In $Cs_2Na[Fe(CN)_6]$ and $Cs_2K[Fe(CN)_6]$ the contribution of the cation charges to the electric-field gradient will be dominated by the Cs^+ cations as these are more irregular than the Na^+ or K^+ cations. Approximate estimates of this ' lattice ' term have been made and suggest that it may well be significant.

The ' valence ' contribution is determined by the relative magnitudes of the spin–orbit coupling constant and the ligand-field splitting. The comparatively strong temperature-dependence observed confirms that the ligand field is non-cubic, but the overall splitting is much less than that of $K_3[Fe(CN)_6]$ in both cases. At 100 K the splittings in $Cs_2Na[Fe(CN)_6]$ (Δ 0.261 $\pm$ 0.003 mm s^{-1}) and $Cs_2K[Fe(CN)_6]$ (0.266) are almost identical, but at 293 K corresponding values are 0.138 and 0.194 mm s^{-1}. The most obvious explanation is that both the ligand-field splitting and the ' lattice ' contribution are markedly different and probably of opposite sign. A full analysis of the data is hampered by the low symmetry of the ligand field, and the difficulties experienced in understanding the data for $K_3[Fe(CN)_6]$ apply equally to those for the new compounds.[1,19–21] A more detailed analysis is therefore inappropriate at the present time. However, $Cs_2Li[Fe(CN)_6]$ has been shown to be a good ' prototype ' material for the t_{2g}^5 configuration in O_h symmetry.

We thank Dr. B. Sheldrick, Department of Biophysics, for use of the diffractometer, and Dr. W. S. McDonald for useful discussions.

[6/1287 *Received*, 2*nd July*, 1976]

[18] T. C. Gibb, *J. Chem. Soc.* (*A*), 1968, 1439.
[19] Y. Hazony, *J. Phys.* (*C*), 1972, **5**, 2267.
[20] F. De S. Barros and W. T. Oosterhuis, *J. Phys.* (*C*), 1970, **3**, L79.
[21] G. Lang and B. W. Dale, *J. Phys.* (*C*), 1973, **6**, L80.